

Simulation of multiphase physico-chemical processes occurring in an orographic hill cap cloud during the FEBUKO field campaign



H. Herrmann, A. Tilgner and Z. Majdik

Leibniz-Institut für Troposphärenforschung, Permoserstr. 15, 04318 Leipzig, Germany

Introduction

A hill capped cloud passage experiment has been modeled by means of the SPACCIM model framework. The measurement took place within the FEBUKO field campaign in October 2001 and 2002 in the Thuringian Forest. Measurements were made at three sampling stations, in the village of Goldlauter (upwind station), at the summit station Schmücke and in Gehlberg (downwind station). Simulations were made with an air parcel traveling along a trajectory from Goldlauter across the orographic cloud to Goldlauter.

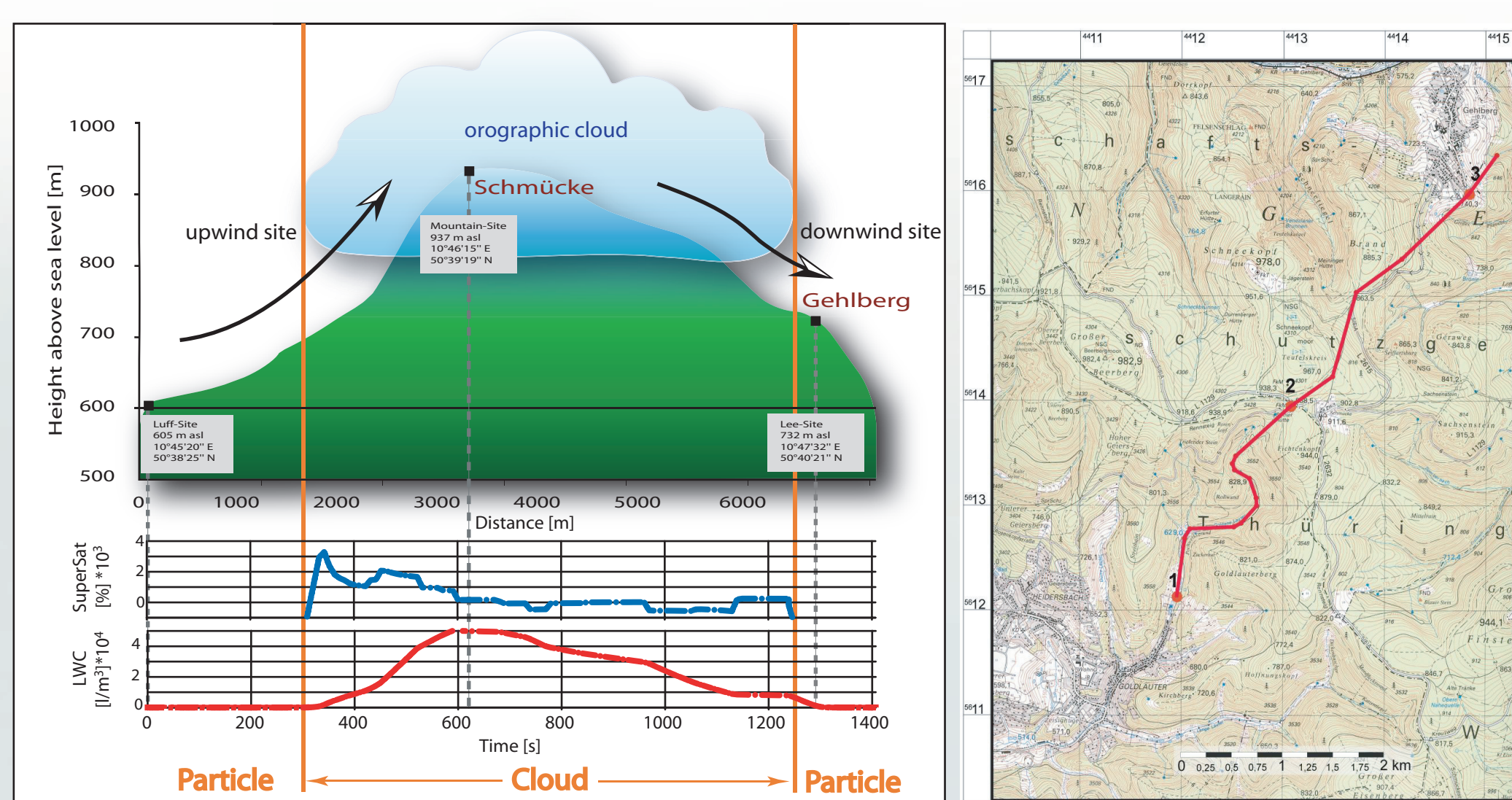


Figure 1: Investigation area: topographic profile and region map with the trajectory (red line).

The goal of the simulations was to investigate the multiphase chemistry occurring in orographic clouds and to understand the incorporation and transformation of atmospheric trace constituents. Simulation results have been compared with cloud water measurements at the summit and impactor measurements at the downwind station in order to interpret the experimental data and for validation of the multiphase chemistry model. In total, 14 cloud events were investigated. Out of these, three events were selected based on detailed analysis of meteorological conditions. Within this analysis we investigated the existence of a connected flow between the three sampling stations. Along with the synoptic situation also regional meteorological data was analyzed to verify the ability of the air mass arriving at the upwind site to overflow the rim.

Model description and initialization

Within SPACCIM complex multiphase chemistry was coupled to a detailed microphysical model. The applied explicit aqueous phase radical mechanisms currently consists of CAPRAM 2.3 (Herrmann et al., 2000) and CAPRAM 2.4 (MODAC-mechanism, Ervens et al., 2003). The gas phase chemistry is described by the regional atmospheric mechanism RACM (Stockwell et al., 1997). Phase transfer processes are treated by means of the resistance model of Schwartz considering Henry's equilibrium, gas phase diffusion and mass accommodation coefficients. For the simulations a fine resolved particle spectrum is considered. A total number of 64 size bins are considered, where multiphase chemistry is considered in droplets where the LWC exceeds $1 \cdot 10^{-12} \text{ l m}^{-3}$. In the next future a feedback from the chemistry to the microphysics will also be implemented. The model was initialized in the particle phase based on measurements with a five stage Berner impactor and a DMPS (Differential Mobility Particle Sizer, Figure 3). In the case of the cloud event on the 27-th of October 2001, most of the mass was found on the third impactor stage (Figure 2), which collects aerosol particles with a diameter between $0.42 \mu\text{m}$ and $1.2 \mu\text{m}$. Nitrate, sulfate, ammonium, organic and elementary carbon are the main components of the aerosol. In the case of chloride and nitrate in order to correct losses encountered by the Berner impactor data from the Steam Jet sampler were used and distributed over the impactor stages analogical to measurements made with the Berner impactor. The initialization of dicarboxylic acids is based on impactor and spray collector measurements. To calculate the water mass of the Goldlauter wet aerosol growth factors were used. The used growth factors were measured during the ACE2 campaign, and are in a good agreement with the measured growth factors by a HTDMA analyzer within the FEBUKO field campaign.

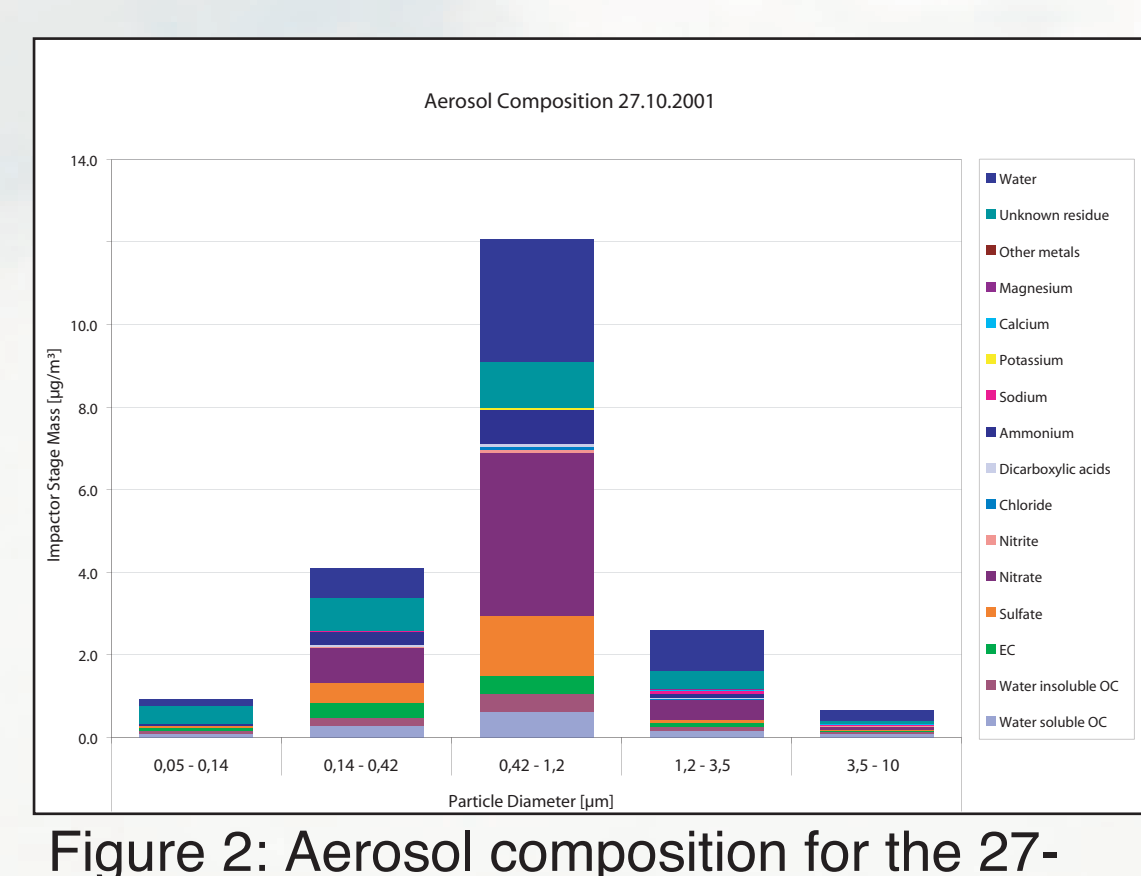


Figure 2: Aerosol composition for the 27-10-2001

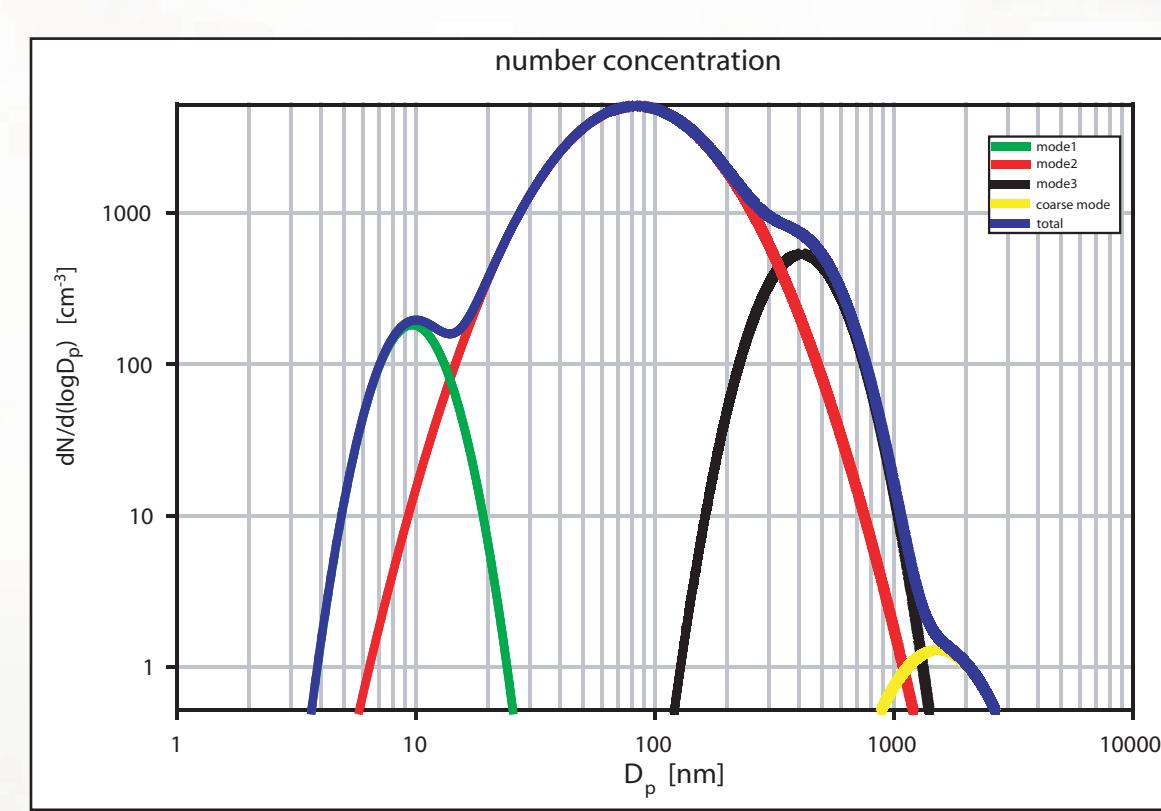


Figure 3: Measured particle number distribution and calculated coarse mode

In the gas phase NO , NO_2 , O_3 and SO_2 were continuously measured, every 5 seconds, using commercially available instruments. For the measurement of HNO_2 and HNO_3 the wet effluent diffusion denuder technique was used. The measured organic species were implemented as stand alone species or were lumped together into special groups as used in the regional atmospheric chemistry mechanism RACM. For some unmeasured species initial concentrations were adopted from the urban CAPRAM standard scenario (MODAC final report) due to the good correlation between measurements and the above mentioned scenario. Based on the experiments a realistic transport time between Goldlauter and Schmücke of 10-20 minutes resulted, depending on meteorological conditions. For the initial wind speed data from the measurement site of the German weather service station located in Meiningen was used. For the cloud event on the 27th of October 2001 at 9.00 UTC an initial wind speed of 4 m s^{-1} was applied, which led to a simulation time of about 23 minutes from the upwind station to the downwind

Simulation results

Simulations carried out with CAPRAM 2.4 for the above mentioned cloud event showed that around 9.00 UTC a coexistence of a night time chemistry, controlled by the NO_3 radical, and a day time chemistry, controlled by the OH radical, exists (Figure 4). The nitrate radical in the gas phase, before and after the cloud reaches a concentration of about $3 \cdot 10^7 \text{ molec. cm}^{-3}$. In the presence of the cloud the NO_3 concentration in the gas phase decreases to about $1 \cdot 10^7 \text{ molec. cm}^{-3}$. In cloud conditions the most important sinks for NO_3 are the reactions of NO_3 with NO (about 40%) and NO_2 (about 52%). Direct uptake of NO_3 into the aqueous phase accounts for about 2.5% out of the total sink processes in the gas phase. The OH radical has a very similar concentration profile. The gas phase concentration in the presence of the cloud decreases with a factor of two from about $6 \cdot 10^4 \text{ molec. cm}^{-3}$ to $3 \cdot 10^4 \text{ molec. cm}^{-3}$. In the gas phase, in cloud conditions, the most important sinks of OH are the reactions with NO_2 (28%), CO (17%), Xylene (15%), Isoprene (14%) and Formaldehyde (2.5%). Phase transfer of OH into the droplets has a contribution of about 2.5% to the total sink. Also, in cloud conditions the OH concentration decreases due to a decrease with a factor of five of the source concentration flux from the reaction of HO_2 with NO . This strong decrease appears due to efficient uptake of HO_2 in the aqueous phase. The most important sinks of OH in the aqueous phase are the reactions with hydrated formaldehyde and formate. During activation, before cloud conditions, the most important sink reactions are the reactions with HC_2O_4^- and HSO_4^- .

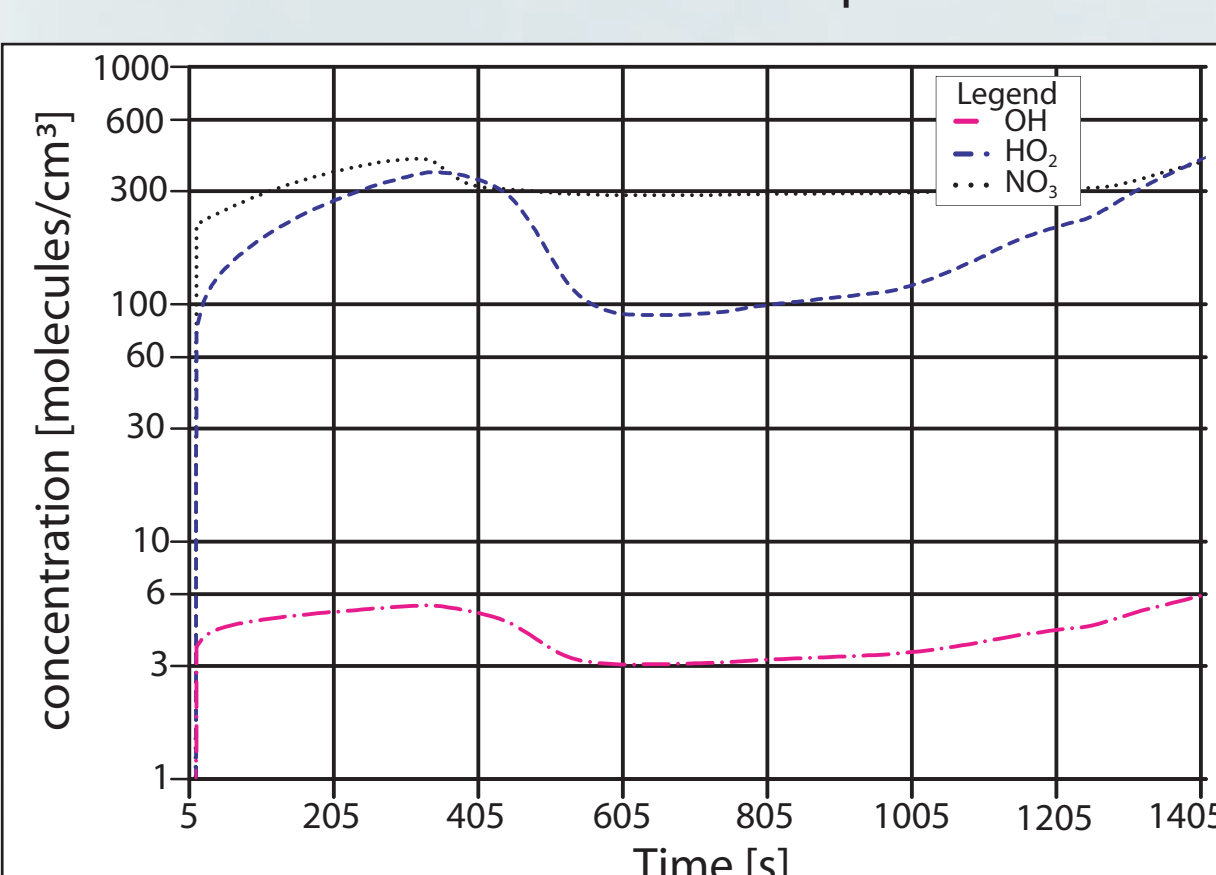


Figure 4: Concentration profile of the OH, HO_2 and NO_3 radicals in the gas phase

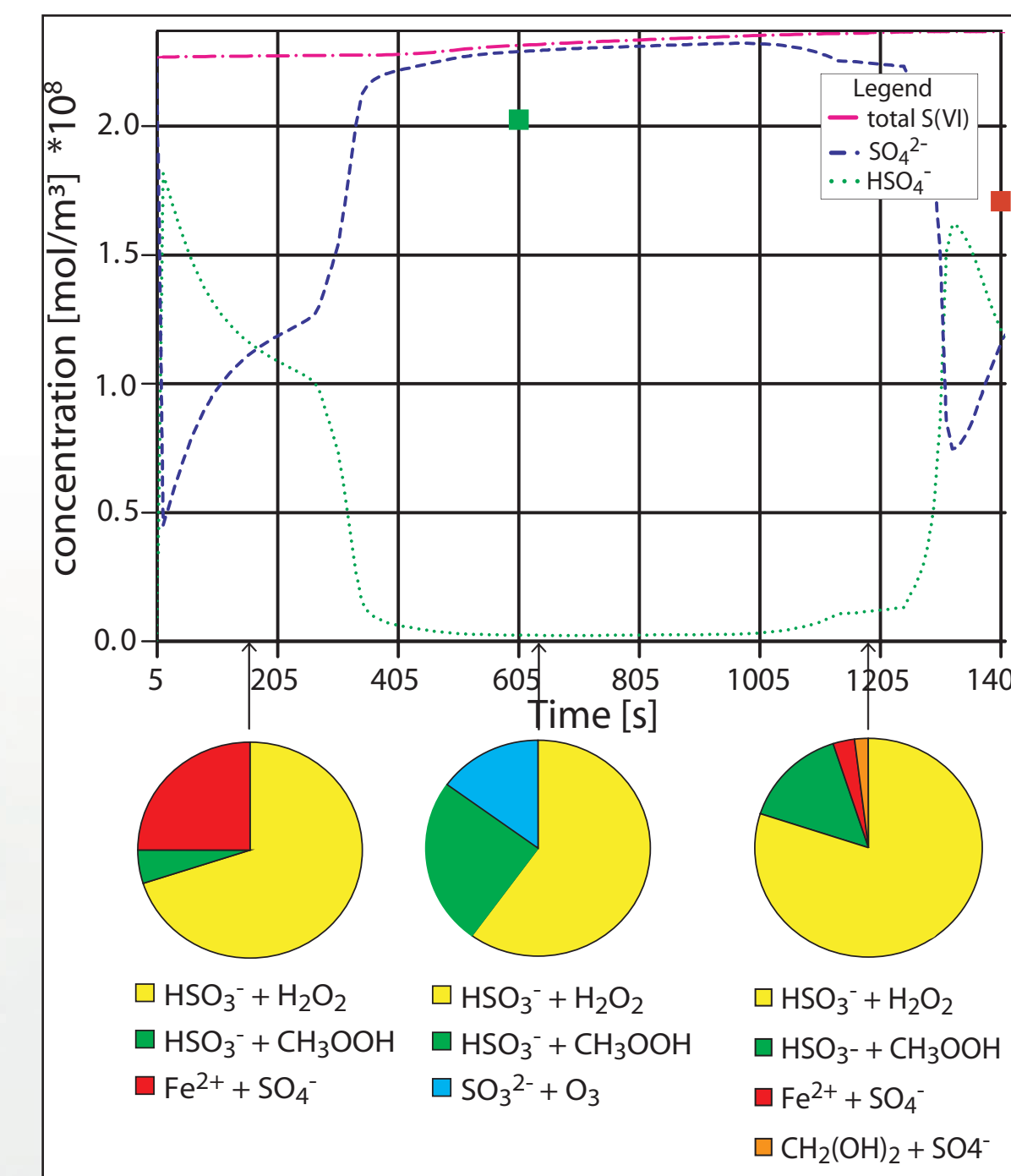


Figure 5 contains the concentration profile of SO_4^{2-} , HSO_4^- and the total S(VI) in function of simulation time. During cloud conditions S(VI) mostly is found in the form of SO_4^{2-} , while in the acidic particles HSO_4^- is predominant. From the upwind to the downwind station a sulfate production of about 4% was modeled. Sulfate production proceeds mainly via the oxidation of bisulfite by hydrogen peroxide, representing about 60%-80% out of the total source of sulfate. Another important source of sulfate is the oxidation of bisulfite by organic peroxides (about 5%-25%). A radical oxidation pathway including transition metal ions seems to be especially important at the beginning of the simulation, before the air parcel enters into the orographic cloud, accounting for about 25% out of the total source. A comparison between measurements and simulation results at the summit station Schmücke showed in general a relatively good agreement. The observed pH value of 4.2 is exactly reproduced by the model. In the case of nitrate and sulfate the measured concentration is with a factor of 1.1 higher than the simulated concentration. In the case of iron the measured concentration is with a factor of 6.8 higher than the simulated value. According to model results about 70% of iron is found in the form of Fe(III).

Figure 5: SO_4^{2-} and HSO_4^- concentration profile, comparison between measurement and simulation results at the summit and the downwind station, the green and the red square representing the experimentally determined

In the case of many organics, roughly a factor two difference between the measured and calculated concentrations exists, e.g. Glyoxal, Oxalate, Acetic acid. In Figure 6 the size-resolved concentration profile of HC_2O_4^- between the upwind and downwind station is showed. The concentration is related to 1 m^3 of air. The highest concentration occurs during activation and at the earlier stages of the orographic cloud in droplets with a diameter between $4 \mu\text{m}$ and $12 \mu\text{m}$. After the summit, oxalate distributes over a wider size-range, consequently the concentration decreases in the individual droplets.

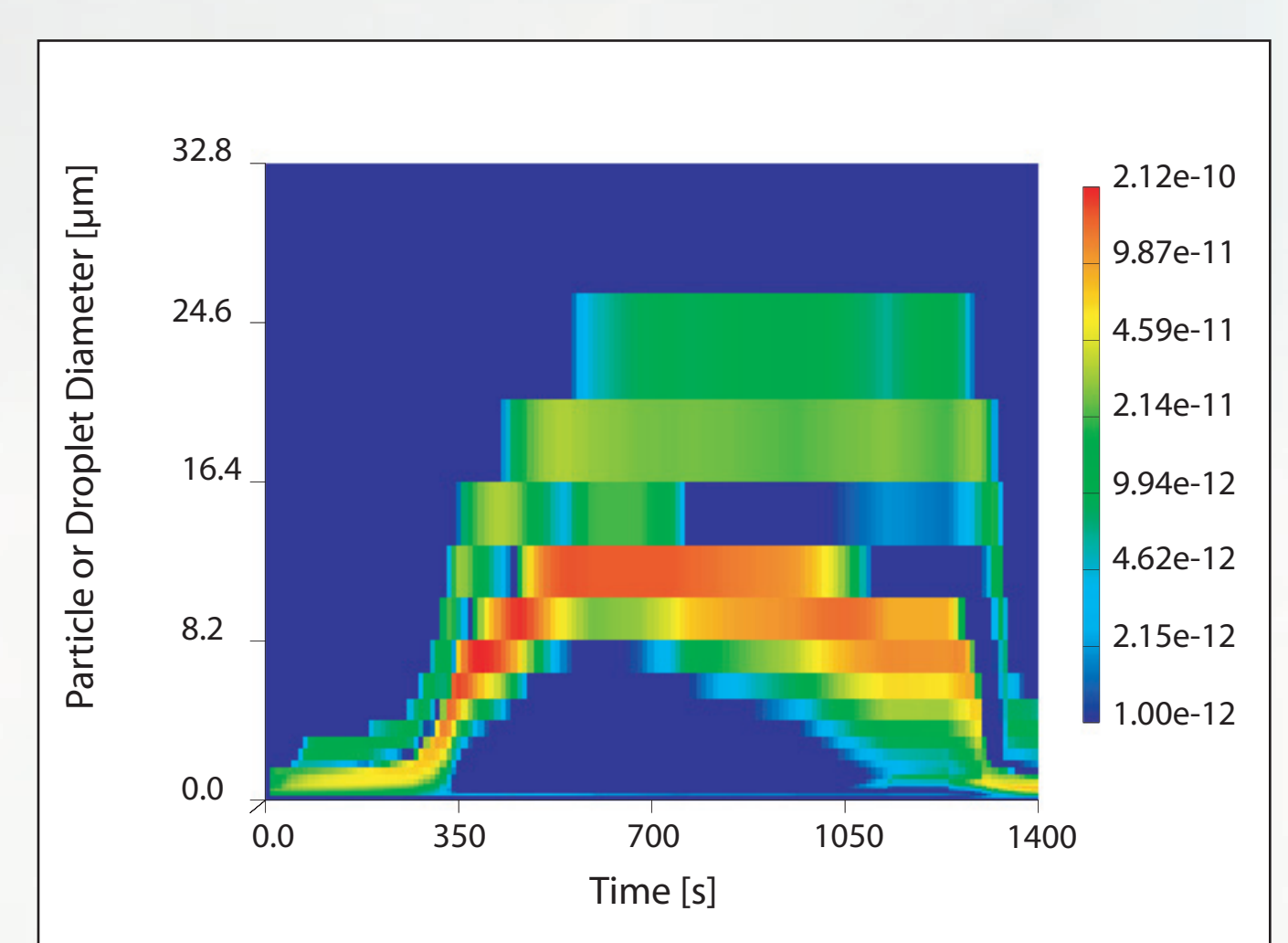


Figure 6: Size and time dependent concentration profile of the oxalate monoanion in mol m^{-3}

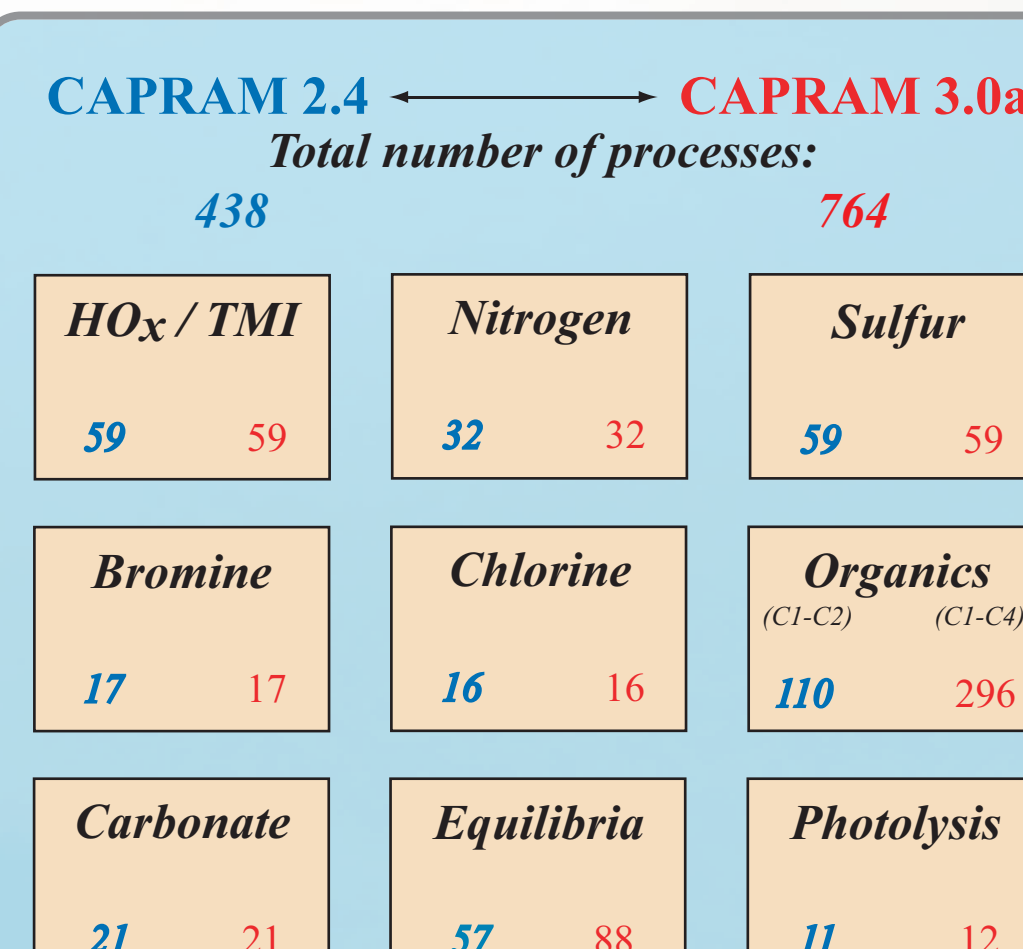


Figure 7: A comparative overview over CAPRAM 2.4 and CAPRAM 3.0 a

In detail CAPRAM 3.0 a considers the oxidation, initiated by the OH radical, of Glyoxalate, 1-Propanol, Propionaldehyde, Propionic acid, Propionate, 2-Propanol, Acetone, Hydroxy Acetone, Hydrated Methylglyoxal, Malonic acid, Malonate (dianion), Malonate (monoanion), Pyruvic acid, Pyruvate, Succinic acid, Succinate (dianion), Succinate (monoanion), Lactic acid, Lactate, Glycolic acid, Glycolate, Acetic acid hydroperoxide, Acetate hydroperoxide, 1-Butanol, Butyraldehyde, Butyraldehyde (hydrated form), Butyric acid, Butyrate, 2-Butanol, Methyl Ethyl Ketone, 2,3-Butanedione, 1,4-Dioxo Butene, 2-Hydroxy 3,4-Dioxo Butyraldehyde, 2-Hydroxy 3,4-Dioxo Butyric acid, 2-Hydroxy 3,4-Dioxo Butyrate, 2,3-Dihydroxy 4-Oxo Butyraldehyde, 2,3-Dihydroxy 4-Oxo Butyric acid, 2,3-Dihydroxy 4-Oxo Butyrate, Ethylene Glycol, Glycolaldehyde, Glycolaldehyde (hydrated form), 3-Hydroxy Pyruvic acid, 3-Hydroxy Pyruvate, 3-Oxo Pyruvic acid, 3-Oxo Pyruvate, Malic acid, Malate, Oxalacetic acid, Oxalacetate, Tartronic acid, Tartarate, Methyl Isobutyl Ketone, Ethyl Formate, N Methyl Pyrrolidinone. Figure 8 contains the oxidation pathway of 1-Propanol implemented in CAPRAM 3.0 a.

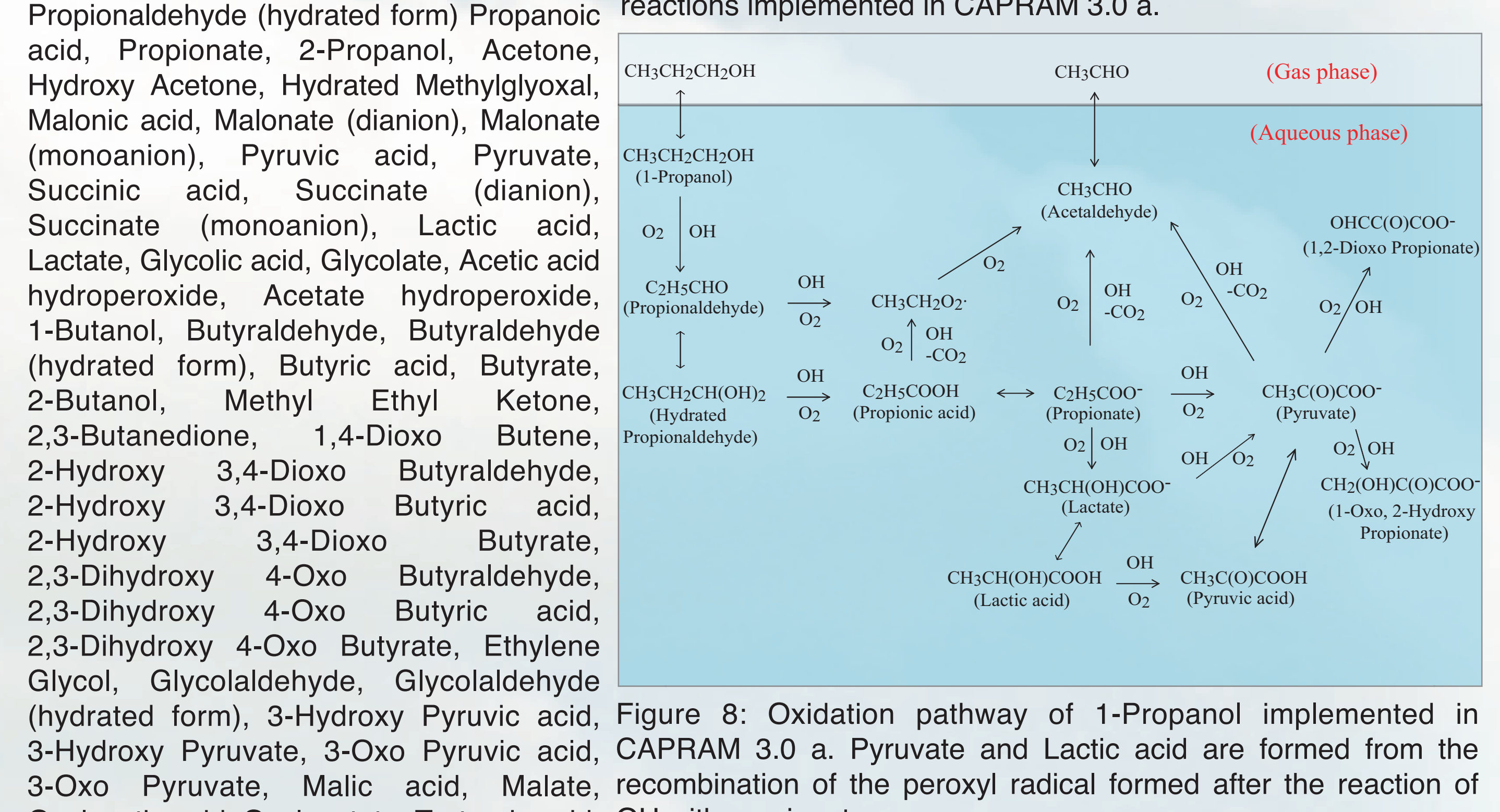


Figure 8: Oxidation pathway of 1-Propanol implemented in CAPRAM 3.0 a. Pyruvate and Lactic acid are formed from the recombination of the peroxy radical formed after the reaction of OH with propionate.

Summary and Outlook

- Simulations of a hill capped cloud experiment were carried out considering detailed microphysics and complex multiphase chemistry
- A comparison at the summit station showed a good agreement between measurements and simulation results
- The chemical mechanism was further extended for a better description of organic chemistry occurring in cloud droplets and aerosol particles
- In the next future the revised and extended chemical mechanism CAPRAM 3.0 will be coupled to detailed microphysics for a more microphysical-chemical models can be detailed analysis of chemical conversions occurring during the critical for a correct interpretation of cloud experiment passage experiments.